A better model for membrane study: Mapping the effects of SOPC in a quaternary phase diagram

Vinisha Garg

Department of Chemistry and Chemical Biology
Honors Thesis
May 9, 2008

Laboratory of Gerald Feigenson, Ph.D.
Department of Molecular Biology and Genetics
Cornell University, Ithaca, NY 14853 USA

KEYWORDS
Electroswelling, fluorescence microscopy, giant unilamellar vesicle (GUV), lipid, phase diagram, SOPC

ABSTRACT
In my study, I attempt to create a unique and more biologically relevant model of the cholesterol-rich exoplasmic leaflet of animal plasma membranes. Using electroswelling to create giant unilamellar vesicles, fluorescence microscopy, and the previously completed ternary mixture of DOPC, DSPC, and cholesterol, DOPC, a rare biological lipid, was gradually replaced with SOPC, an abundant biological lipid in order to create a partially completed quaternary phase diagram consisting of DOPC, SOPC, DSPC, and cholesterol. Focusing on the biological raft region, (L_o+L_α coexistence phase), reduction in the size of the coexistence region was found, thus verifying the notion that SOPC is more miscible with DSPC and cholesterol than is DOPC. DOPC replacements greater than 70% resulted in a disappearance of the coexistence region leading to a suspicion that the phase domains were too small to observe using optical fluorescence microscopy. The creation of a more biological model membrane can be used to further understand the role of lipids and proteins in cellular membranes as well as the size of biological rafts important in cellular function.

1. Introduction

Biological membranes are composed of numerous lipids and proteins in both the exoplasmic and cytoplasmic leaflets that are essential for many aspects of cellular function[1]. For this reason, plasma membranes deserve intense study. Evidence suggests that animal plasma membranes consist of a heterogeneous mixture of lipid and protein components that are non-randomly distributed throughout the bilayer[2]. The many membrane components have distinct thermodynamic mixing properties and thus interact differently with each other. Some components within the exoplasmic leaflet, such as cholesterol and sphingolipids, aggregate into fluid bilayer domains, termed "rafts" (**Figure 1a**).

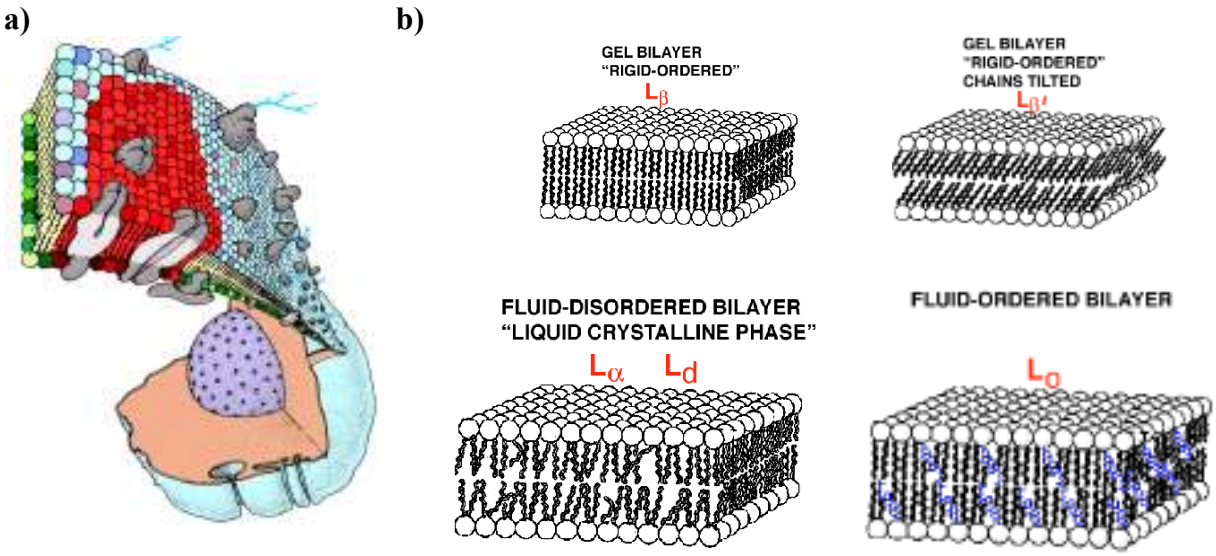

Figure 1. a) This cartoon shows an animal cell membrane in which many proteins and phospholipids are embedded. The phospholipids are non-randomly distributed throughout the membrane as shown by the cluster of lipids in red that have aggregated into a particular phase. **b)** The two types of phases include gel and fluid. The gel phases, L_β and L_β' (tilted chains, not biologically relevant), have rigid acyl chains, and the membrane lipids cannot move around easily. In the liquid disordered, L_α, phase, acyl chains have significant local motion, and the entire lipid molecules can diffuse easily. The cholesterol-rich phase, L_o (liquid ordered), differs from L_α in that the acyl chains are highly ordered, similar to a crystal.

The membrane raft hypothesis describes the lateral organization of lipids due to the preferential packing of cholesterol and sphingolipids into domains, which serve as an attachment point for specific proteins[3]. Rafts correspond to a liquid-ordered (L_o) phase[4] of the lipids that are more tightly packed than other non-raft liquid domains (L_α) (**Figure 1b**). The tighter packing is entropy-driven because nonpolar cholesterol relies on polar phospholipid headgroups for coverage in order to avoid the unfavorable free energy of cholesterol contact with water[5]. Usually, saturated phospholipids can pack better around cholesterol than can phospolipids with unsaturated hydrocarbon chains[6].

The physical and chemical properties of biological membranes, specifically the tendency of membrane components to cluster and form distinct phase regions, have been proposed to play an essential role in many biological processes. For example, recent work has established that lipid rafts play a role in cell endocytosis, virus budding from host cells, receptor signaling for immune processes, initiation of hormone signaling cascades, protein stabilization, protein and lipid sorting, and membrane fusion[7-8]. (**Figure 2**).

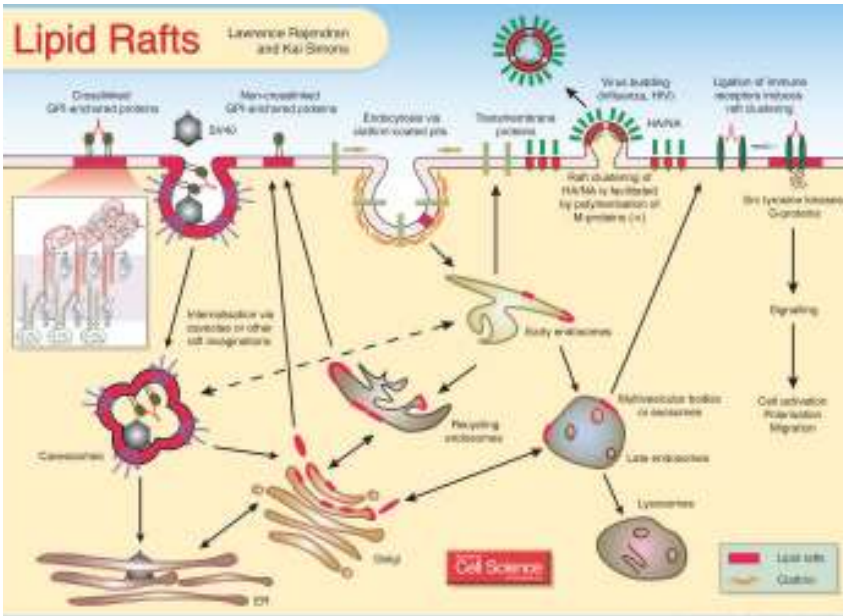

Figure 2. Depiction of the multiple functions of rafts in biological membranes[7].

Membrane phase behaviors have been difficult to investigate in real plasma membranes due to the large number of lipid components and their asymmetric, or unlike, distribution between the exoplasmic and cytoplasmic leaflets[9-11]. For this reason, artificial membranes with well-defined chemical components are used to model phase behavior in cells. By determining the thermodynamic phase diagrams of ternary lipid mixtures, a better understanding of membrane phase behavior can be achieved. Recent work has been done with synthetic membranes using ternary mixtures consisting of DOPC (an unsaturated lipid), DSPC (a saturated lipid), and Chol (cholesterol)[12] (**Figure 3a**).

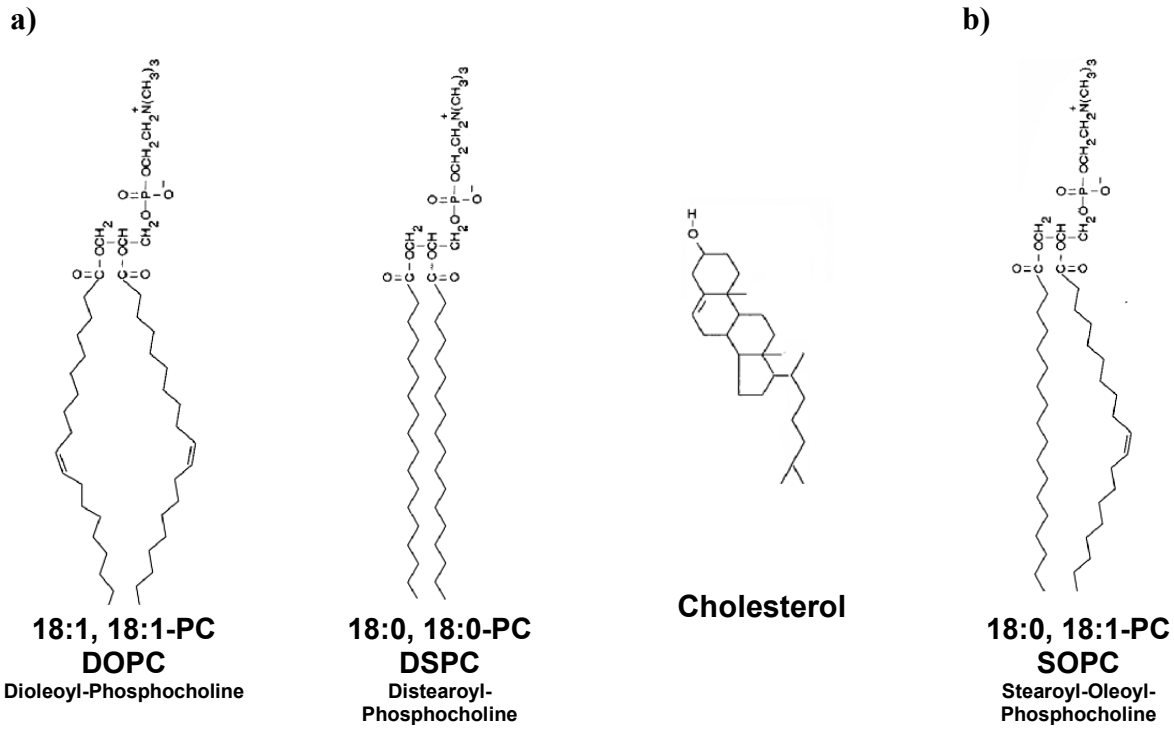

Figure 3. a) Structures of relevant phospholipids and cholesterol. The two double bonds in the DOPC chains result in relatively unfavorable mixing with DSPC and cholesterol. DSPC is fully saturated and can tightly pack around cholesterol, which has a small polar head. **b)** Note one double bond in SOPC compared to two double bonds in DOPC.

The DOPC/DSPC/Chol phase diagram has been completed and verified using four distinct methods of phase boundary determination[12]: fluorescence microscopy to

visualize giant unilamellar vesicles (GUVs) at equilibrium, fluorescence resonance energy transfer[13], fluorescence of dilute dyes[14], and X-ray diffraction. This ternary system was used as a model of non-random mixing of lipids due to the mixing and packing properties of the lipids. Specifically, the two unsaturations of DOPC cause immiscibility with the saturated DSPC, which can pack tightly around cholesterol. This mixture results in a large and clearly-defined region of two-phase liquid coexistence (L_o+L_α phases). However, while the non-random mixing of these lipids provides an accurate phase diagram, its biological relevance is minimal due to the rarity of DOPC in mammalian plasma membranes[15].

I aim to improve our current model for animal cell plasma membranes by making the model lipid system more biologically relevant. As a result, my task has been to gradually replace DOPC with SOPC, a singly unsaturated lipid (**Figure 3b**), which is abundant within the exoplasmic leaflet of mammalian cell plasma membranes[15]. Using fluorescence microscopy and the formation of artificial membrane bilayers, GUVs, formed via "electroswelling"[16] (see Methods), I have been able to construct a partially completed quaternary phase diagram, a feat that is unique to my laboratory. With over 90 reliable GUV compositions, I focused on the liquid-liquid coexistence region due to its relevance in understanding biological raft domains (L_o and L_α regions)[4].

Since SOPC has one fewer unsaturation than DOPC, we expected that SOPC would mix more favorably with DSPC and cholesterol than does DOPC. This would result in a smaller two-phase coexistence region (L_o and L_α) on an SOPC/DSPC/Chol phase diagram. At high replacement of DOPC with SOPC (>70%) however, I found that the phase boundary determined from fluorescence microscopy images of GUVs (between

the one-phase and two-phase liquid regions) disappeared altogether. To investigate this finding further, lipid mixtures with fixed cholesterol percentages were made to better observe the way in which the boundary disappeared in the quaternary diagram. The experimental strategy behind this was to select a composition of lipids that was well into the two-phase coexistence region (L_o+L_α) in the ternary diagram and then vary SOPC to find what percentage of DOPC must be replaced before the GUVs no longer appeared phase-separated. These data were plotted on a quaternary phase diagram (computer code was written in Mathematica by a graduate student in our lab, Frederick Heberle) to locate the shifts in the previously established ternary boundary lines.

2. Experimental

2.1 Materials

The phospholipids (DOPC, SOPC, and DSPC dissolved in chloroform) were purchased from Avanti Polar Lipids, Inc (Alabaster, AL); cholesterol was purchased from Nu-Chek Prep, Inc (Elysian, MN); and the fluorescent dyes 1,1'-dieicosanyl-3,3,3',3'-tetramethylindocarbocyanine perchlorate (C20:0-DiI) (**Figure 4a**), 2-(4,4-difluoro-5,7-dimethyl-4-bora-3a,4a-diaza-s-indacene-3-pentanoyl)-1-hexadecanoyl-*sn*-glycero-3-phsphocholine (16:0, Bodipy)-PC (**Figure 4b**), and 1,1'-didodecyl-3,3,3',3'-tetramethylindocarbocyanine perchlorate (C12:0-DiI) (**Figure 4c**) were purchased from Invitrogen (Eugene, OR). Dyes were selected based on previously determined partitioning behaviors[12].

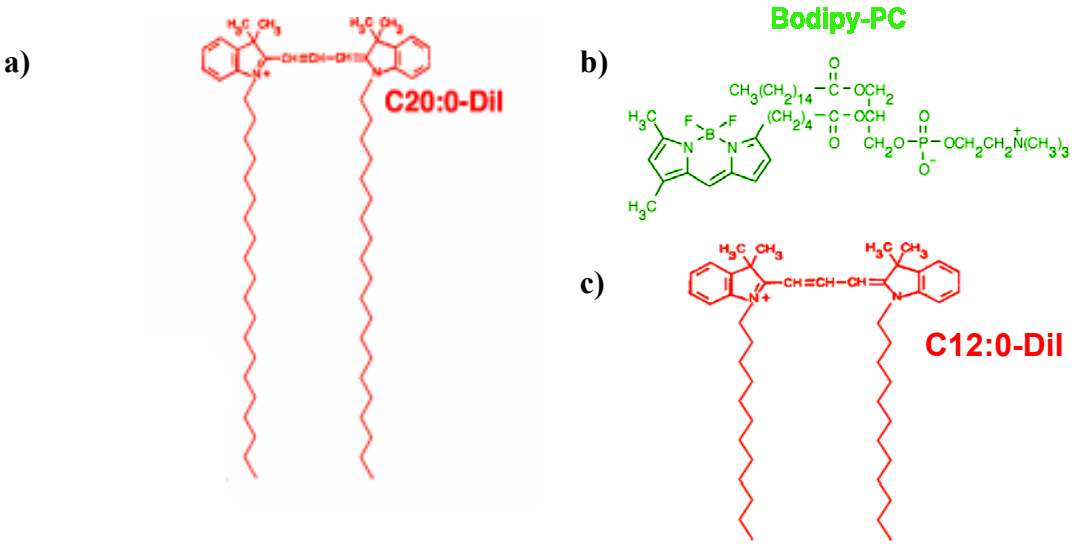

Figure 4. Structures of fluorescent probes. **a)** C20:0-DiI partitions into the Lo phase because its long, saturation chains pack well in the liquid ordered phase. **b)** (16:0, Bodipy)-PC partitions into the Lα phase. **c)** C12:0-DiI partitions into the Lα phase because its chains and short and favorably mixes in the disordered phase.

Purity of lipids was confirmed by thin-layer chromatography (TLC) on washed, activated (run in chloroform/methanol 1/1 solvent) Adsorbosil TLC plates (Alltech, Deerfield, IL). The TLC slides were developed with chloroform/methanol/water (65/25/4) for all phospholipids, chloroform/methanol (9/1) for C20:0-DiI, and petroleum ether/diethyl ether/chloroform (7/3/3) for cholesterol analysis. All solvents used were HPLC grade. Phospholipid stocks were quantified by phosphate assays[17] regularly. Cholesterol stocks were prepared analytically. The fluorescent dye stocks were quantified by absorption spectroscopy using an HP 8452A spectrophotometer (Hewlett-Packard, Palo Alto, CA). Extinction coefficients (Invitrogen, Eugene, OR) used were 143,000 M^{-1} cm^{-1} at 549nm for C20:0 Di-I, 91,800 M^{-1} cm^{-1} at 504nm for (16:0, Bodipy)-PC, and 144,000 M^{-1} cm^{-1} at 549nm for C12:0-DiI.

2.2 Methods

Artificial bilayers, or giant unilamellar vesicles (GUVs), of several compositions were made by a method called "electroswelling"[16]. This method allows for the production

of GUVs with diameters of 15-50 μm (**Figure 5**). Each sample contained a 300 nmol mixture of lipids (SOPC, DOPC, DSPC, Chol), 200 μl of chloroform as the solvent, and fluorescent probes in a dye:lipid mole ratio of 1:3000. After trying multiple experiments with different dye ratios, this dye percentage was found not to affect phase behavior of the vesicles for the experiment. Each mixture was then carefully and evenly spread onto two polished, indium tin oxide (ITO)-coated microscope slides (Delta Technologies, Stillwater, MN) on a hotplate set at 54°C to evaporate the chloroform. The slides were then placed in a desiccator under high vacuum for 1 hour to remove residual chloroform. The slides were then heated to 65°C, a Buna o-ring was placed on the spread lipid mixtures on the slide, a 100mM sucrose solution was added into the O-ring, and another duplicate mixture slide placed on top to seal the o-ring, thus forming a chamber for vesicle formation. The slides were then incubated for 2 hours at 65°C with an AC field of 5 Hz, ± 1 V (pulse/function generator, WAVETEK, San Diego, CA) to produce GUVs. After 2 hours, the temperature was ramped down to 23°C over a period of 6-8 hours.

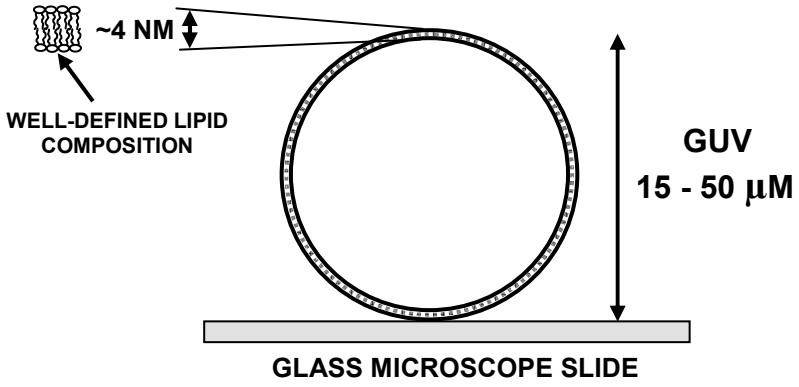

Figure 5. Depiction of a single GUV, an artificial bilayer, on an indium tin oxide microscope slide. Average size of vesicles is between 15-50μm. Note: Phase behavior results are not dependent on GUV size.

The solution was then harvested (collected) from the slide and placed into an Eppendorf tube. 5 μl of the GUV/sucrose solution was placed on a glass microscope slide within a ring of Apiezon N Grease (M&I Materials, LTD, Manchester, UK) and then enclosed by a no. 1 coverslip for observation at an ambient temperature of ~23°C. Fluorescence microscopy (Nikon Diaphot-TMD Inverted Microscope, Melville, NY) with a 100W short arc mercury lamp (Osram, Germany) and a 70x water immersion objective (LUMO) was used to visualize the GUVs[18-20]. Observations of GUVs were made through the eyepiece with excitation filters set at red 540-550 nm for C20:0-DiI and C12:0-DiI (Filter Set 41003, Chroma Tech. Corp) and green 460-500 nm for (16:0, Bodipy)-PC (Filter Set 41001, Chroma Tech. Corp). GUV images were captured with a high sensitivity Sensys CCD camera with 768x512 imaging array, 9x9 μm pixels (Photometrics, Tucson, AZ). The vesicles in each mixture were then characterized as phase-separated, due to the appearance of coexisting phases, or uniform, due to no visible coexisting phases. The black-and-white pictures were then colorized using Adobe Photoshop 7.0 (San Jose, CA) to make the vesicles appear as they did in the microscope. The contrast and color were slightly altered in order to make the domains more visible.

Background (Terminology)

In the following experiments, DOPC is replaced with SOPC. Replacement percentages will be written as 50% replacement, 60% replacement, 70% replacement, etc. 50% replacement of DOPC by SOPC means that for a given molar lipid composition of DOPC/DSPC/Chol (ex. 0.4/0.2/0.4), 50% of the mole fraction of DOPC is replaced by SOPC (ex. 0.2/0.2/0.2/0.4 = DOPC/SOPC/DSPC/Chol). In this example, 50% of the original mole fraction of DOPC (0.4) is replaced with SOPC, resulting in a mole fraction

of 0.2 for DOPC and a mole of fraction of 0.2 for SOPC. I refer to this lipid composition as xPC/DSPC/Chol = 0.4/0.2/0.4 with a 50% replacement of DOPC by SOPC. xPC is the mole fraction of DOPC+SOPC. All ratios and compositions are molar ratios.

3. Results

With the detailed phase diagram for the ternary lipid mixture DOPC/DSPC/Chol (**Figure 6**), we have a large and well-defined liquid coexistence (L_α + L_o) region and single liquid phase regions (L_α , L_o)[12].

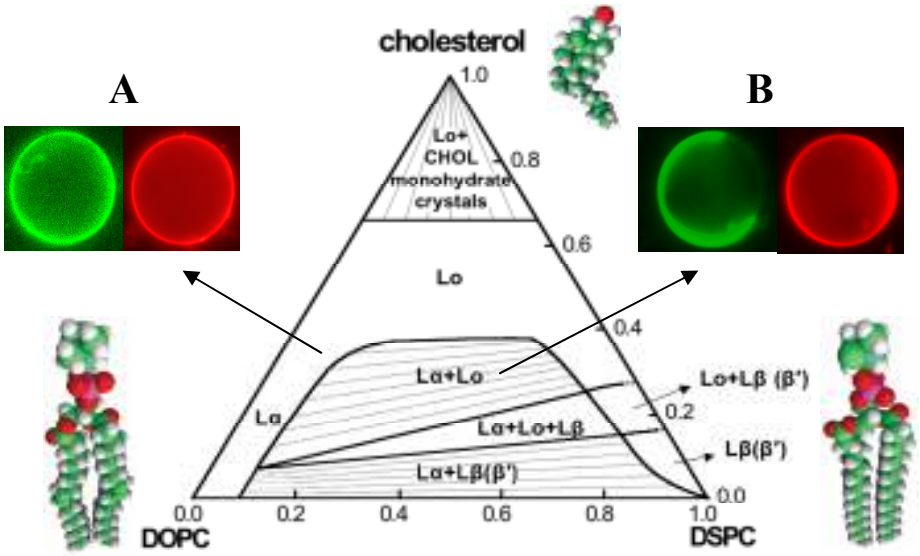

Figure 6. Ternary phase diagram of DSPC/DOPC/Chol with the space filling models of the lipids. Each vertex of the triangle represents 100% of the noted lipid. The line opposite to the vertex represents 0% of the lipid. The triangle contains all possible compositions of the three components. Uniform vesicles (A) in the one-phase liquid regions are shown. Phase-separated vesicles (B) in the two-phase coexistence region are shown. The phase-separated vesicles show probes that complementarily partition into separate phases (one in L_o and the other in L_α). Vesicles are lit with (16:0, Bodipy)-PC (vesicles in green) and C20:0-DiI (vesicles in red).

Two compositional series of samples along straight lines, or "trajectories", were completed. One trajectory, shown as the blue arrow in **Figure 7a**, was designed to go through the left part of the phase boundary at a constant xPC(DOPC+SOPC):Chol mole ratio of 7:3 while varying the DSPC percentage and using C20:0-DiI and (16:0, Bodipy)-

PC. GUV images for that trajectory (**Figure 7b**) at 10% intervals of SOPC replacement ranging from 50-70% replacement of DOPC with SOPC show the boundary line between uniform (L_α region) and phase-separated (L_o+L_α region) vesicles shifting, thus forming a smaller two-phase coexistence (L_o+L_α) region. 50% replacement was used as a starting point because previous study of this quaternary system indicated that 50% replacement showed a shift in the phase boundary. At 70% replacement however, the boundary seems to disappear, thus all vesicles appear uniform all the way into the two-phase region at 41% DSPC lipid composition (shown only to 26% DSPC in **Figure 7b**).

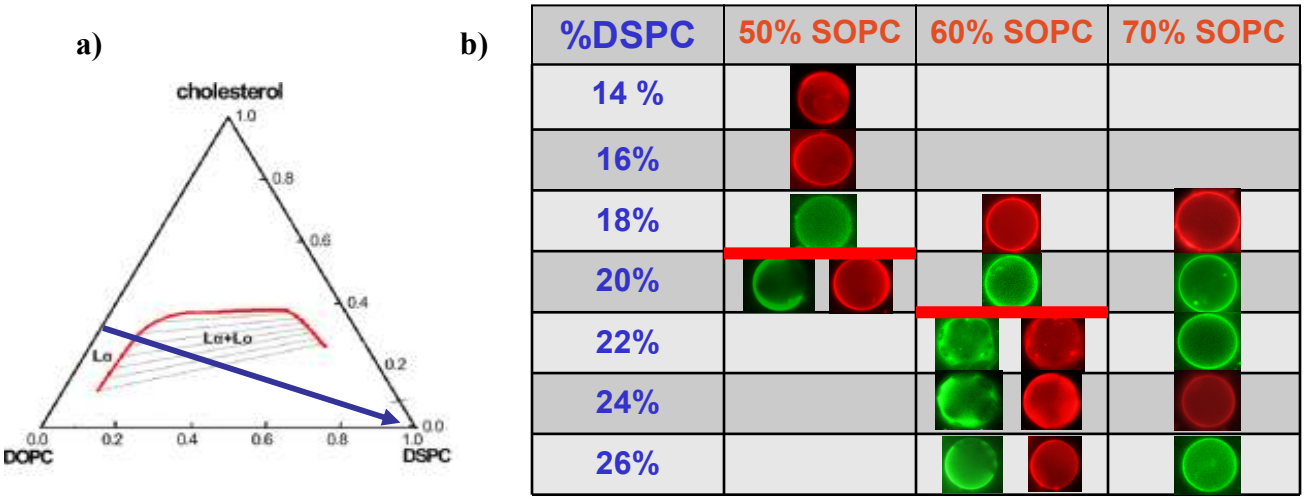

Figure 7. a) Diagram of the DOPC/DSPC/Chol liquid-liquid coexistence region. The blue arrow indicates a constant xPC:Chol mole ratio of 7:3 and varying DSPC percentages. Moving along the arrow to the vertex increases the DSPC percentage in the compositions. The boundary of liquid-liquid coexistence at 0% replacement of DOPC is at 9% DSPC (point where blue line intersects the red phase boundary line). **b)** GUV images of compositions along the blue line in Figure 7a. Compositions contain C20:0-DiI and (16:0, Bodipy)-PC in a dye:lipid mole ratio of 1:3000. The columns (in red) are replacement of DOPC with SOPC. The rows (in blue) represent the percentage of DSPC in the lipid composition at the fixed xPC:Chol ratio. Red lines indicate a phase change from one-phase to two-phase coexistence looking at the pictures from top to bottom. At 50% replacement of DOPC by SOPC, the boundary shifts from 9% DSPC to roughly 19% DSPC. At 60% SOPC replacement, boundary shifts farther inward to 21% DSPC. At 70% replacement, the boundary disappears, resulting in only uniform vesicles even after going as far into the two-phase region as 41% DSPC (shown only to 26% on figure).

The second trajectory was through the middle part of the phase boundary at a constant DOPC:DSPC ratio of 1:1 with a varying cholesterol percentage using C12:0-DiI (**Figure 8a**). The change in dye is not significant to phase boundary results. GUV images for that trajectory (**Figure 8b**) for 0%, 33%, and 67% replacement of DOPC with SOPC again show the boundary line between uniform (one-phase region) and phase-separated (two-phase region) vesicles shifting, thus forming a smaller two-phase coexistence (L_o+L_α) region. The disappearance of the phase boundary was not observed because the SOPC replacement of DOPC was not greater than 70%, which is the point at which the boundary disappeared in the first trajectory.

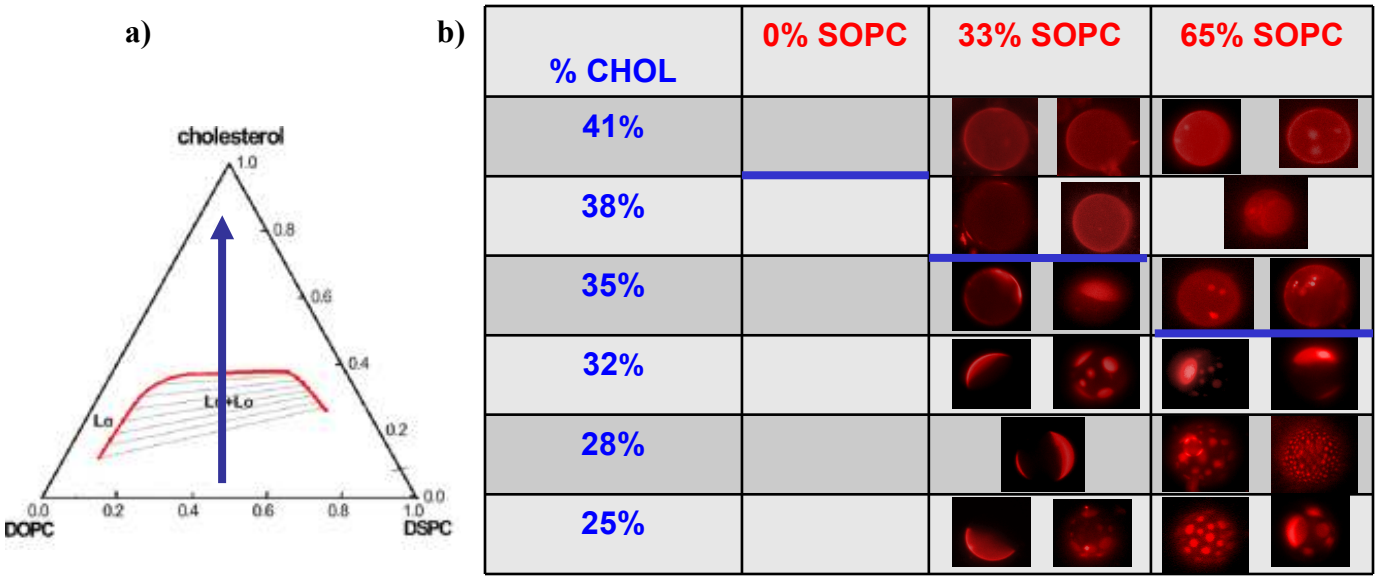

Figure 8. **a)** Diagram of the DOPC/DSPC/Chol liquid regions. The blue arrow indicates a constant xPC:DSPC ratio of 1:1 with varying Chol percentages. Moving along the arrow to the vertex increases the Chol percentage in the compositions. The liquid-liquid coexistence boundary at 0% replacement of DOPC is at 39.5% Chol (point where blue line intersects the red phase boundary line). **b)** GUV images of compositions along the blue line in Figure 8a. Compositions contain C12:0-DiI in a dye:lipid mole ratio of 1:3000. The columns (in red) are replacement of DOPC with SOPC. The rows (in blue) represent the percentage of Chol in the lipid composition at the fixed xPC:DSPC ratio. Blue lines indicate a phase change from one-phase to two-phase coexistence looking at the pictures from top to bottom. At 33% replacement of DOPC with SOPC, the boundary shifts from 39.5% Chol to 36.5% Chol. At 67% SOPC replacement, boundary shifts farther inward to 33.5% Chol.

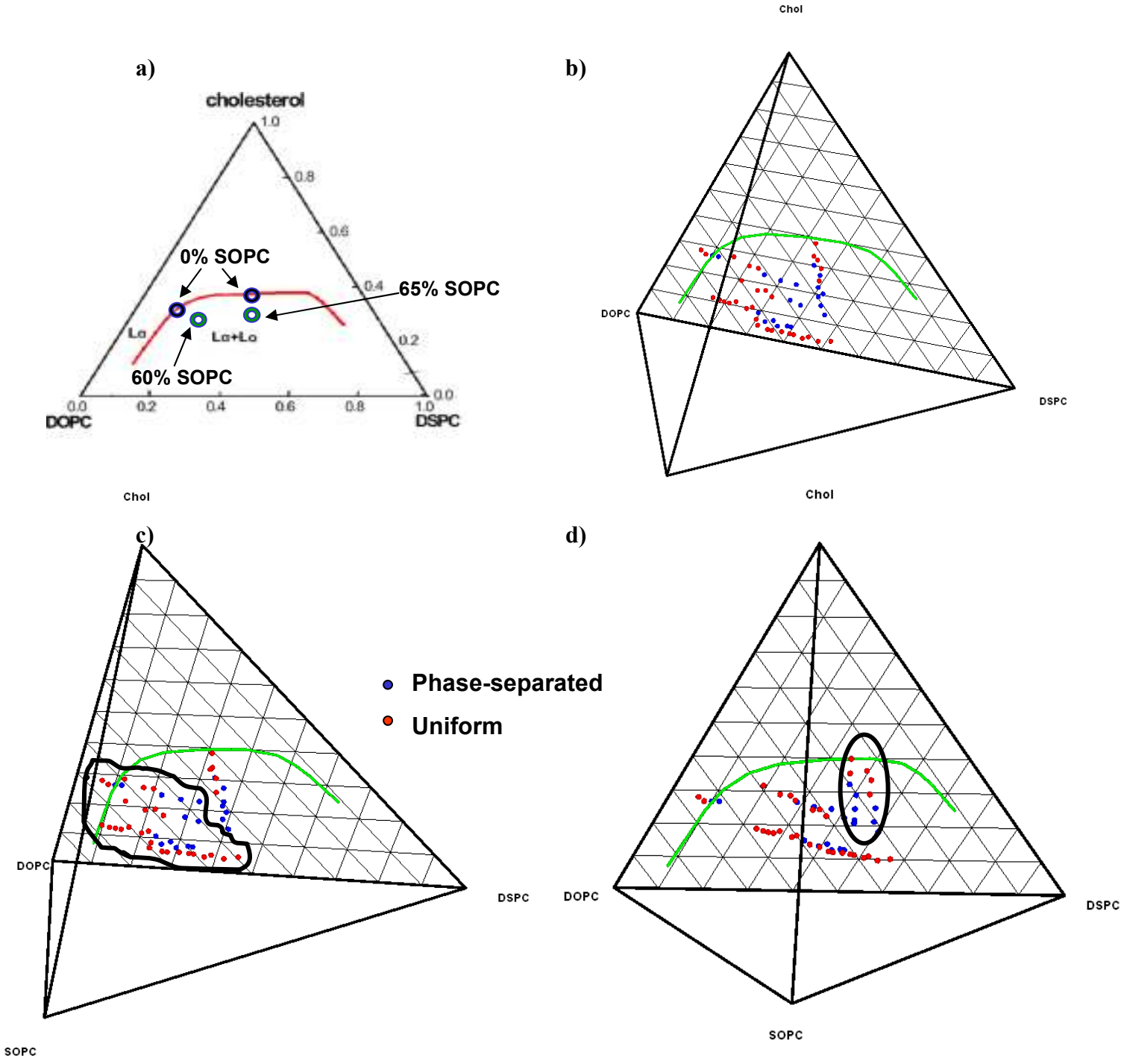

Figure 9. a) Diagram of the DOPC/SOPC/DSPC/Chol liquid regions. The blue circles represent the position of the ternary mixture (0% SOPC in the mixture) and green circles represent movement of that boundary point with the replacement of DOPC with SOPC (60% SOPC replacement for the left trajectory and 65% SOPC replacement for the middle trajectory). Diagram portrays the smaller two-phase region and larger one-phase region with the addition of SOPC. **b)** Quaternary diagram of the two trajectories in **Figures 7a, 8a** DOPC/SOPC/DSPC/Chol. Blue points represent phase-separated vesicles and red points represent uniform vesicles. **c)** Left trajectory of Figure 7a. circled. **d)** Middle trajectory of Figure 8a. circled.

Both trajectories (**Figures 7a, 8a**) showed a decrease in the size of the phase-separated, L_o+L_α region at compositions of less than 70% DOPC replacement by SOPC (**Figure 9a**). The data was plotted on a quaternary phase diagram of DOPC/SOPC/DSPC/Chol (**Figure 9b**). **Figures 9 c,d** show a different viewing angle of the left trajectory and middle trajectory respectively on a quaternary phase diagram.

Two more data sets were obtained while maintaining a fixed cholesterol percentage. In this trajectory, a composition of lipids that was well into the two-phase coexistence region (L_o+L_α) in the ternary diagram was selected and then the SOPC replacement of DOPC was varied to find the percentage of DOPC replacement needed for the liquid domains to disappear (all uniform vesicles). The first set was a trajectory at a fixed 30% cholesterol composition keeping an xPC(DOPC+SOPC):DSPC mole ratio of 1:1 while varying replacement of DOPC in increments of 5% from 50-100% replacement with SOPC (**Figure 10a**). The boundary abruptly disappeared between 70-75% of DOPC replacement with SOPC. The second data set was a set of four trajectories at fixed 25% cholesterol with four different mole ratios of xPC:DSPC (1:1, 3:2, 2:3, and 11:9) while varying DOPC replacement with SOPC in increments of 5% from 60-100%. (**Figure 10b**). All four trajectories showed abrupt disappearance of boundaries between 75-80% DOPC replacement with SOPC.

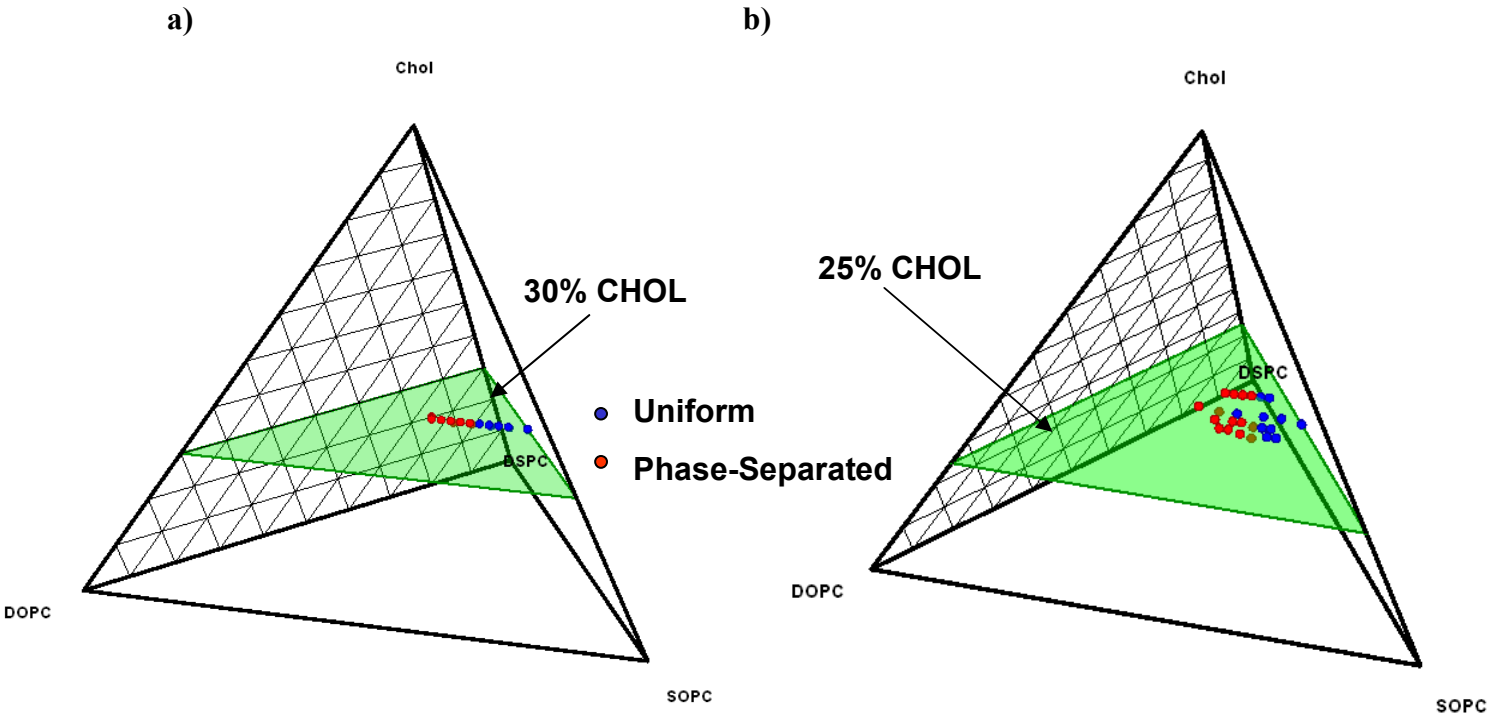

Figure 10. Quaternary diagrams of DOPC/SOPC/DSPC/Chol. Red points are phase-separated vesicles and blue points are uniform vesicles. **a)** Quaternary diagram of trajectory with fixed cholesterol at 30%, 1:1 xPC(DOPC+SOPC):DSPC mole ratio, and varying the replacement percentage of DOPC by SOPC. Shows an abrupt disappearance of phase-separated vesicles between 70-75% replacement of DOPC. **b)** Quaternary diagram of four trajectories with fixed cholesterol at 25%, 1:1, 3:2, 2:3, and 11:9 xPC:DSPC ratios, and varying the replacement percentage of DOPC by SOPC. Three trajectories (3:2, 2:3, and 11:9) showed disappearance of phase-separated vesicles between 70-75% replacement of DOPC. 1:1 trajectory showed a disappearance of phase-separated vesicles between 70-80% replacement of DOPC.

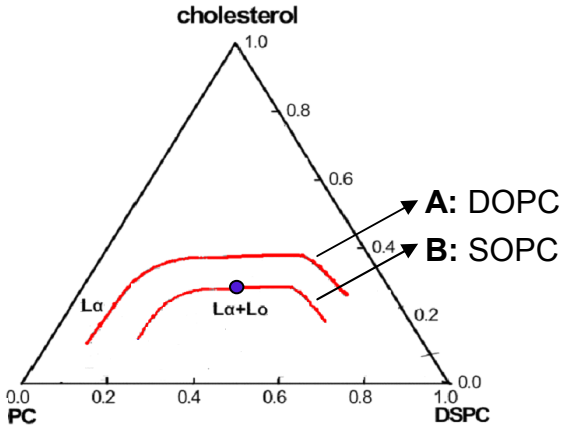

Figure 11: Ternary phase diagram showing liquid-liquid region for DOPC/DSPC/Chol, shown by A, and a proposed ternary phase diagram showing liquid-liquid regions for SOPC/DSPC/Chol, shown by B, based upon FRET data. The point in blue shows the phase boundary for a mole ratio of 1:1 SOPC:DSPC at 30% cholesterol.

4. Discussion

One strategy for studying the phase behavior of biological membranes is to construct model systems and analyze their phase behaviors. The most complex membrane models that have been published are ternary mixtures containing cholesterol[21-22], but due to the numerous different lipids that compose biological membranes, a quaternary phase diagram is more representative of actual membranes. Construction of quaternary phase diagrams is challenging.

We propose the strategy of generating a quaternary phase diagram based on observing phase boundary shifts that occur in a well-established ternary diagram, namely the DOPC/DSPC/Chol mixture, with the addition of a fourth component. Even though it is rare in biological membranes, DOPC was previously chosen because of its relatively unfavorable interactions with cholesterol and DSPC due to its two double bonds. This unfavorable mixing results in macroscopic L_o and L_α phase separation over a large region of compositions.

Using GUVs and fluorescence microscopy has been advantageous in studying phase boundaries. By using fluorescent dyes that selectively partition into specific liquid domains, the micron-scale domains that represent distinct phase regions within a vesicle are directly visible. Individual GUVs for a given lipid composition contain different domain sizes and domain area fractions, thus determination of phase behavior is based on a majority of vesicles. Roughly 20-30 vesicles were examined for each composition. GUVs with compositions just past the boundary for the two-phase coexistence region exhibit an abrupt disappearance of domains, allowing accurate determination of boundary

locations. The compositional resolution varies with the different trajectories, but we estimate an error of roughly 3%.

The upper boundary, the liquid-liquid coexistence or so-called “raft region”, was the focus of my work since it is the region that is most clearly observable by fluorescence microscopy and is most relevant for biological systems. By gradually replacing the DOPC component with SOPC and tracking the movement of the phase boundary, I have found phase shifts as well as a disappearance of the boundary line altogether. This strategy appears to be reliable and shows great potential in investigating other fourth components, such as glycolipids or proteins.

The quaternary mixture DOPC/SOPC/DSPC/Chol is presented here as a model for the exoplasmic leaflet of animal plasma membranes. The abundance of SOPC in biological membranes makes this quaternary mixture an important improvement in the biological relevance of the previous model. As expected by the presence of a single unsaturation, SOPC does show more favorable mixing with the saturated DSPC and cholesterol than DOPC, as evidenced by the narrowing of the two-phase coexistence region. Since SOPC has only one double bond, it was expected to be more miscible with DSPC and cholesterol. The two double bonds in DOPC limit its miscibility with the other lipid components. The left boundary and middle boundary shifts were consistent with one another and showed a smooth transition of the phase boundary line, with the exception of the high DOPC replacement where the boundary disappears altogether (discussed further below). In other words, with incremental DOPC replacement, the two-phase coexistence region seemed to smoothly diminish in size. The data strongly suggest that SOPC is more

miscible with DSPC and cholesterol, thus resulting in a larger one-phase liquid region and a smaller two-phase region.

Also interesting were the results pertaining to the disappearance of domains at high (>70%) replacement of DOPC by SOPC. The boundary disappeared as seen by the five trajectories at fixed cholesterol percentages (**Figure 10a, b**). Fluorescence resonance energy transfer (FRET) is a method of finding phase boundary locations with better resolution[13], and was used to verify the GUV results and to provide additional information. FRET experiments showed a phase boundary at high SOPC percentages, namely 100% SOPC. Using FRET data, the liquid-liquid phase boundary for a ternary mixture of SOPC/DSPC/Chol was proposed (**Figure 11**). At a mole ratio of 1:1 SOPC:DSPC, the liquid-liquid coexistence phase boundary was found at 30% cholesterol (**Figure 11**) (Shih Lin Goh, unpublished). Images of GUVs with high SOPC replacement compositions showed uniform fluorescence with no visible domains. This corresponds to a disappearance of the boundary that describes *macroscopic* phase coexistence. GUV analysis can reliably detect only micrometer-sized domains[22-24] while FRET can detect nanometer-sized domains[25-27]. A possible explanation for the difference between GUV and FRET data is that the phases have separated, but the domain size is smaller than the wavelength of the light. Such small domains can be called "nanodomains", and are not detectable by optical fluorescence microscopy. Hence, the GUVs appear uniform[21]. If in fact nanodomain sized rafts, L_o regions within the fluid membrane, exist in mammalian plasma membranes, then proteins could potentially play a role in organizing the small raft domains. Perhaps proteins must aggregate and cluster these small domains in order to create platforms to execute functions in membrane trafficking and signaling[3].

The different mixing properties of membrane lipids give rise to phase-separated domains. The boundary lines acquired for the quaternary phase diagram will be used to find the lipid-lipid microscopic interaction energies by Monte Carlo simulations[28]. These studies can help in understanding the mixing abilities of membrane proteins with different lipids, which can provide insight into the rules that govern protein partitioning in liquid phases[29]. By building these quaternary phase diagrams and determining the underlying molecular interactions, specifically lipid and protein mixing properties that induce formation of raft regions, we will be able to understand the roles of the enormous variety of lipids and proteins in mammalian plasma membranes.

5. Conclusion

By gradually replacing DOPC with the natural lipid SOPC in the previously established ternary mixture of DOPC/DSPC/Chol, I have detected a gradual decrease in the size of the two-phase (L_o+L_α) coexistence region. This observation is consistent with the structure of SOPC, specifically its one double bond, which can mix better with the saturated DSPC and cholesterol than can DOPC, with its two double bonds. Additionally, I have found that at high SOPC replacement of DOPC (>70%), there is disappearance of the boundary line in a tetrahedral depiction as shown by **Figure 10 a,b**. FRET data suggests the presence of nanodomains, which are not visible in GUV images under a fluorescence microscope. The possibility of nanometer-sized raft domains in biological membranes could imply that proteins play a large role in aggregating and organizing these small regions. Raft-binding proteins may be significant in coupling small raft

domains in membranes to create a larger functional raft region, which can then play important roles in cellular processes[3,30].

After completing the quaternary diagram of DOPC/SOPC/DSPC/Chol, a more biological model system, calculation of interaction energies by Monte Carlo Simulations[21] can be performed in an effort to understand the molecular interactions between membrane lipids. We will be able to eventually describe multi-component lipid and protein mixtures, perhaps even mixtures as complex as biological plasma membrane components. By studying the formation of rafts within membranes, we are getting closer to understanding the biological application of rafts in virus interaction, hormone signaling, endocytosis, exocytosis, and immune receptor signalling[3].

Acknowledgements

I would like to thank my research advisor Gerald W. Feigenson for his guidance, Frederick A. Heberle, Shih Lin Goh, Nelson F. Morales, Jiang Zhao, Jing Wu, Robin Smith, Julie Lin, and Michelle Zeng for help in mapping the phase diagrams, technique training, and relevant scientific discussions. This research was supported by grants from the NIH and the NSF.

References

1. van Meer, G. 2005. Cellular lipidomics. *EMBO Journal* 24 (18): 3159-3165.

2. Simons, K. and van Meer, G. 1988. Lipid sorting in epithelial cells. *Biochemistry* 27: 6197-6202.

3. Simons, K. and Ikonen, E. 1997. Functional rafts in cell membranes. *Nature* 387 (6633): 569-572.

4. Brown, D.A. and London, E. 1998. Structure and origin of ordered lipid domains in biological membranes. *Journal of Membrane Biology* 164: 103-114.

5. Huang, J. and Feigenson, G.W. 1999. A Microscopic Interactoin Model of Maximum Solubility of Cholesterol in Lipid Bilayers. *Biophysical Journal* 76 (4): 2142-2157.

6. Simons, K. and Vaz, W.L. 2004. Model systems, lipid rafts, and cell membranes1. *Annual Review of Biophysics and Biomolecular Structure* 33: 269-295.

7. Rajendran, L. and Simons, K. 2005. Lipid rafts and membrane dynamics. *Journal of Cell Science* 118 (6): 1099-1102.

8. Brown, D.A. and London, E. 1998. Fuctions of lipid rafts in biological membranes. *Annual Review of Cell and Developmental Biology* 14: 111-136.

9. Op den Kamp, J.A.F. 1979. Lipid asymmetry in membranes. *Annual Review of Biochemistry* 48: 47-71.

10. Roelofsen, B. and Op den Kamp, J. A. F. 1994. Plasma membrane phospholipid asymmetry and its maintenance: The human erythrocyte as a model. *Current Topics in Membranes* 40: 7-46.

11. Daleke, D. L. 2003. Regulation of transbilayer plasma membrane phospholipid asymmytry. *The Journal of Lipid Research* 44 (2): 233-242

12. Zhao, J., Wu, J., Heberle, F.A., Mills, T.T., Klawitter, P., Huang, G., Costanza, G., and Feigenson, G.W. 2007. Phase studies of model biomembranes: Complex behavior of DSPC/DOPC/Cholesterol. *Biochimica et Biophysica Acta* 1768: 2764-2776.

13. Loura, L.M.S., Fedorov, A., and Prieto, M. 2001. Fluid-fluid membrane microheterogeneity: a fluorescence resonance energy transfer study. *Biophysical Journal*. 80: 776-788.

14. Heberle, F.A., Buboltz, J.T., Stringer, D., and Feigenson G.W. 2005. Fluorescence methods to detect phase boundaries in lipid bilayer mixtures. *Biochimica et Biophysica Acta* 1746: 186-192.

15. Gennis, R.B. 1989. *Biomembranes: molecular structure and function*. New York: Springer-Verlag.

16. Angelova, M.I., Soleau, S., Meleard, P., Faucon, J.F., and Bothorel, P. 1992. Preparation of giant vesicles by external AC electric fields. Kinetics and applications. *Progress in Colloid and Polymer Science* 89: 127-131.

17. Kingsley, P.B. and Feigenson, G.W. 1979. The Synthesis of a Perdeuterated Phospholipid: 1,2-Dimyristoyl-*sn*-Glycero-3-Phosphocholine-d72, *Chemistry and Physics of Lipids* 24: 135-147.

18. Schneider, M. B., Jenkins, J. T., and Webb, W. W. 1984. Thermal fluctuations of large cylindrical phospholipid vesicles. *Biophysical Journal* 45: 891–899.

19. Akashi, K., Miyata, H., Itoh, H. & Kinosita, K. 1996. Preparation of giant liposomes in physiological conditions and their characterization under an optical microscope. *Biophysical Journal* 71: 3242–3250.

20. Moscho, A., Orwar, O., Chiu, D. T., Modi, B. P., and Zare, R. N. 1996. Rapid Preparation of Giant Unilamellar Vesicles. *Proceedings of the National Academy of Sciences of the United States of America* 93: 11443–11447.

21. Feigenson, G.W. and Buboltz, J.T. 2001. Ternary phase diagram of dipalmitoyl-PC/dilauroyl-PC/cholesterol: Nanoscopic domain formation driven by cholesterol. *Biophysical Journal* 80: 2775-2788

22. Veatch, S. L. and S. L. Keller. 2003. Separation of liquid phases in giant vesicles of ternary mixtures of phospholipids and cholesterol. *Biophysical Journal* 85: 3074-3083.

23. Dietrich, C. et al. 2001. Lipid rafts reconstituted in model membranes. *Biophysical Journal* 80: 1417-1428.

24. Baumgart, T., Hess, S.T., and Webb, W.W. 2003. Imaging coexisting fluid domains in biomembrane models coupling curvature and line tension. *Nature* 425: 821-824.

25. Loura, L.M.S., de Almeida, R.F.M, and Prieto, M. 2001. Detection and characterization of membrane microheterogeneity by resonance energy transfer. *Journal of Fluorescence* 11: 197-209.

26. de Almeida, R.F.M., Loura, L.M.S., Fedorov, A., and Prieto, M. 2005. Lipid rafts have different sizes depending on membrane composition: a time-resolved fluorescence resonance energy transfer study. *Journal of Molecular Biology* 346: 1109-1120.

27. Towles, K.B., Brown, A.C., Wrenn, S.P., and Dan, N. 2007. Effect of Membrane Microheteroheneity and Domain Size on Fluorescence Resonance Energy Transfer. *Biophysical Journal* 93: 655-667.

28. Huang, J. 2002. Explorations of molecular interactions in cholesterol superlattices: Effect of multibody interactions. *Biophysical Journal* 83: 1014-1025.

29. Huang, J. and Feigenson, G.W. 1999. A microscopic interaction model of maximum solubility of cholesterol in lipid bilayers. *Biophysical Journal* 76: 2142-2157.

30. Gri, G.,Molon, B., Manes, S., Pozzan, T. and Viola, A. 2004. The inner side of T cell lipid rafts. *Immunology Letters* 94: 247-252.